Indian J Phys (April 2024) 98(4):1343–1353
https://doi.org/10.1007/s12648-023-02917-3

ORIGINAL PAPER

Investigation of structural, electronic, magnetic, elastic and thermodynamic properties of $Mn_2Cr_{1-x}V_xSi$ (x = 0, 0.25, 0.5, 0.75 and 1) alloys

A İyigör[1], O Örnek[2]*, A Saydam[2] and N Arıkan[3]

[1]Department of Machinery and Metal Technology, Kırşehir Ahi Evran University, Kırşehir, Turkey

[2]Department of Materials and Metallurgical Engineering, Kırşehir Ahi Evran University, Kırşehir, Turkey

[3]Department of Medical Services and Techniques, Osmaniye Korkut Ata University, Osmaniye, Turkey

Received: 09 March 2023 / Accepted: 17 August 2023 / Published online: 13 September 2023

Abstract: In this manuscript, the structural, electronic, magnetic, elastic and thermodynamic properties of $Mn_2Cr_{1-x}V_xSi$ (x = 0, 0.25, 0.5, 0.75 and 1) alloys are studied by employing the Quantum Espresso code in the framework of DFT simulations. We have used Perdew–Burke–Ernzerhof's (PBE) generalized gradient approach (GGA) for all the calculations. The optimized lattice constant, bulk modulus and elastic constants of these alloys are predicted and evaluated, and then, shear modulus, Young modulus, Poisson's ratio, Vickers hardness, elastic anisotropy, Debye temperature and melting temperatures are obtained using elastic constants. The brittle/ductile nature and isotropic/anisotropic behaviors of the materials are investigated. By analyzing the B/G ratio, we conclude that all materials except Mn_2VSi are ductile in nature. According to the results of the calculations on the electronic properties of the alloys, it is clearly seen that they have metallic character due to the overlap between the conduction and the valence band at the Fermi level for the spin-up and spin-down states. Finally, thermodynamic properties of $Mn_2Cr_{1-x}V_xSi$ (x = 0, 0.25, 0.5, 0.75 and 1) alloys have been calculated using the quasi-harmonic Debye model by applying stress to the optimized crystal structures. The results indicate that these alloys are promising candidates for high-temperature applications.

Keywords: Elastic properties; Mechanical properties; Density functional theory

1. Introduction

The materials in the Heusler group attract the attention of researchers due to their wide and comprehensive properties. The thermal and electrical properties of new alloys were obtained by using non-ferromagnetic materials together with Heusler type alloys, whose discovery dates to 1903, have been an area of interest for researchers [1]. The ternary intermetallic Heusler alloys have cubic structures, with the stoichiometric combination X_2YZ being the transition metal elements of X and Y and the main group element of Z. The first Heusler alloy was obtained in the $L2_1$ phase Fm-3 m (#225) space group consisting of four fcc sublattices. Over time, as the studies on Heusler type alloys increased, inverse and quaternary Heusler materials joined this family. Inverse Heusler materials can also be obtained in the XA structure (X_2YZ) and are in the F-43 m space group, and quaternary Heusler materials of another Heusler type are in the F-43 m space group with the chemical formula XX′YZ. The LiMgPdSn structure is a prototype for quaternary Heusler type materials [2, 3]. These materials have a wide range of properties such as half-metallic [4–6], thermodynamics [7, 8], shape memory effect [7, 9], heavy fermion behavior [10, 11], magnetic [12, 13] and superconductivity [14]. Materials in the Heusler group generally have high spin polarization. One of the directions of the spins shows metallic properties, while the other shows semiconductor or insulating properties. For this reason, they are classified as semi-metallic materials with magnetic properties.

The alloys in the Mn–V(Cr)–Si system have been investigated such as structural, electronic, magnetic [15–17], formation energy [18] and half-metallic antiferromagnetic properties [19, 20] using different theoretical

*Corresponding author, E-mail: osmanornek@ahievran.edu.tr

© 2023 IACS

and experimental methods. Luo et al. [15] studied the structural, electronic and magnetic properties of Mn_2CrSi alloy by the FLAPW method. In a similar study, Fujii et al. [16] reported the structural, electronic and magnetic properties using the FLAPW method. The experimental structural properties of Mn_2VSi antiferromagnetic thin film using X-ray diffraction (XRD) were determined by Wu et al. [17]. Half-metallic ferrimagnet and structural properties of Mn_2VSi alloy using full potential electronic structure method (FPLO) by Özdoğan et al. [18]. In a similar study, Galanakis et al. [19] studied the antiferromagnetic half-metallic properties of Mn_2CrSi and Mn_2VSi alloys with the FPLO method. Li et al. [20] reported that the *B/G* ratios of Mn_2CrSi and Mn_2VSi alloys were 5.78 and 1.69, respectively, and the Poisson ratios were 0.30 and 0.25, respectively; the research was conducted with the CASTEP package program. Kirklin et al. [21] obtained the formation energy of Mn_2VSi alloy as − 0.516 eV with the VASP package program. Apart from these, Four et al. [22] investigated the electronic structure, magnetic properties and thermal properties of $Cr_2GdSi_{1-x}Ge_x$ half-metallic ferromagnetic full-Heusler alloys using the FLAPW method. The magneto-electronic, mechanical and thermodynamic properties of $Cr_2GdGe_{1-x}Sn_x$ full-Heusler alloy were determined by the FLAPW method by Asfour et al. [23]. The semi-metallic properties of TiXSb (X: Ru, Pt), X_2VSi (X = Ti, Co) and their quaternary TiCoVSi and CoTiVSi compounds were investigated using the FP-LAPW method using different pseudopotentials [24, 25]. Intermetallic alloys applications include magnetic materials, hydrogen storage materials, refractory alloys, high strength materials, metallic glasses, antifriction materials and barrier layers. In addition, they have extensive industrial applications in semiconductors, superconductors, aerospace, furnace hardware and piping of chemical industries [26]. From this point of view, $Mn_2Cr_{1-x}V_xSi$ (x = 0; 0.25; 0.5; 0.75; 1) alloys have been studied by doping various proportions of V atoms to the Mn_2CrSi full-Heusler alloy, which has a limited number of studies in the literature. For instance, the mechanical properties of these alloys have not been adequately defined in previous studies. Elastic properties play an important role in determining the strength and stiffness of a material. Elastic constants are key parameters in describing how the material responds to interatomic forces, electron–phonon interactions, phase transition, and transport coefficients as a function of mass and shear modulus [27]. Because the doping of the V atom to the Mn_2CrSi alloy can also affect the physical properties. The addition of the V atom can cause changes in the crystal structure. It also enables improvements in important properties such as the mechanical strength of this alloy. Therefore, this study aims to investigate the structural, electronic, magnetic and elastic properties of $Mn_2Cr_{1-x}V_xSi$ (x = 0; 0.25; 0.5; 0.75; 1) alloys, obtained by doping various proportions of V atoms to the Mn_2CrSi full-Heusler alloy, using by the plane-wave pseudopotential method.

2. Computational method

To accomplish this work, we obtained the structural, electronic, magnetic and elastic properties of the given alloys by the pseudopotential plane-wave approximation method based on density functional theory (DFT) [28] as implemented in the Quantum Espresso package [29]. We have used the generalized gradient approximation (GGA) in the scheme of Perdew–Burke–Ernzerhof generalized gradient approximation (PBE-GGA) [30] for the exchange and correlation function. First, convergence calculations for the kinetic energy cut-off, K-points and smearing parameter have been determined. Thus, the kinetic energy cut-off was taken as 40 Ry to be used in the calculations, and the smearing parameter was 0.01 Ry according to Methfessel–Paxton [31]. For $Fm\bar{3}m$ and $Pm\bar{3}m$ cubic phases, k-points were used as 8 × 8 × 8 in the total energy calculation and as 12 × 12 × 12 in the density of state calculation, 6 × 6 × 5 in the total energy calculation and 12 × 12 × 10 in the density of states calculation for the P4/mmm tetragonal structure. The elastic constants of the alloys were calculated using the energy-strain method applied to the thermo_pw package [32, 33]. To determine variables such as heat capacity, entropy and vibrational energy, thermodynamic calculations were made using the Debye Model in the thermo_pw package described in Ref. [33].

3. Results and discussions

The x = 0 and 1 states of $Mn_2Cr_{1-x}V_xSi$ (x = 0; 0.25; 0.5; 0.75; 1) alloys, that is, Mn_2CrSi and Mn_2VSi full-Heusler alloys are crystallized in the $Fm\bar{3}m$ space group as shown in Fig. 1a and e. At x = 0.25 and 0.75 cases, $Mn_2Cr_{0.75}V_{0.25}Si$ and $Mn_2Cr_{0.25}V_{0\cdot75}Si$ alloys are formed in the $Pm\bar{3}m$ space group in presented in Fig. 1b and d. On the other hand, for the x = 0.5 states, the $Mn_2Cr_{0.5}V_{0.5}Si$ quaternary tetragonal alloy is crystallized in the P4/mmm space group as in Fig. 1c. The Wyckoff positions of atoms for the three phases have been presented in Table 1.

The calculated equilibrium lattice constants and bulk modulus values of Mn_2CrSi and Mn_2VSi alloys are presented in Table 2 and compared with the available data in the literature [15, 16, 18]. Our results for both alloys are in good agreement with the literature data. There are no

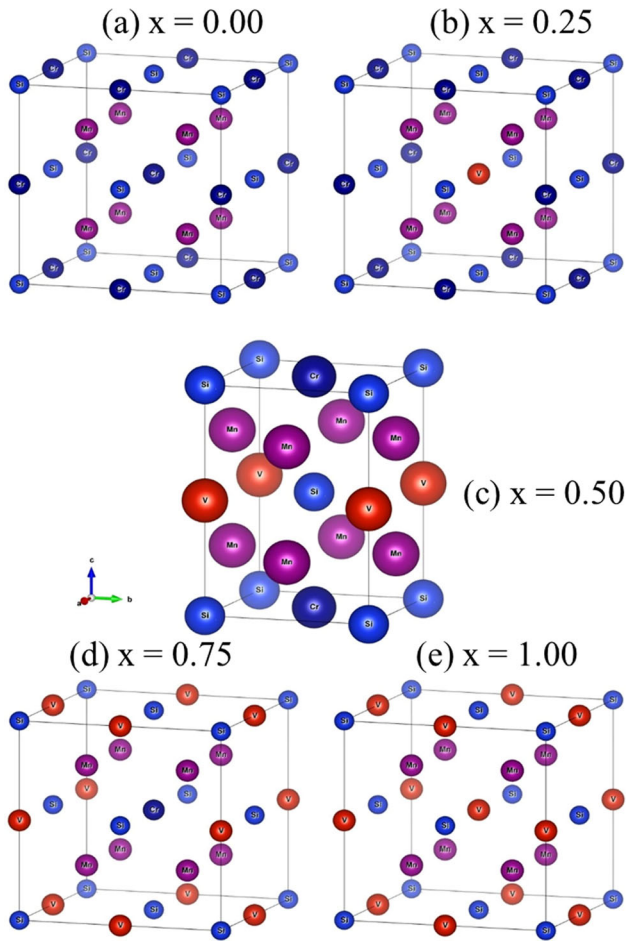

Fig. 1 Crystal structures of $Mn_2Cr_{1-x}V_xSi$ (x = 0; 0.25; 0.5; 0.75; 1) alloys

comparable studies on the other three alloys in the literature. In addition, it is seen from the data in Table 2 that there is an increase in the value of the lattice constant with the increase in the contribution of the V atom. We consider that our herein computed results for the considered alloys are reliable and recommend future experimental studies to confirm our calculated results.

The elastic constants (C_{ij}) of the herein alloys can be computed from the optimized structures using an energy-strain method. Elastic constants play an important role in describing the properties of a material, providing much information such as the anisotropic character of bonding, the binding characteristic between adjacent atomic planes and mechanical stability. Alloys belonging to the $Fm\bar{3}m$ and $Pm\bar{3}m$ space groups and at doping ratios of $x = 0, 0.25, 0.75, 1$ have cubic crystal symmetry. Solid materials in the P4/mmm space group crystallize in tetragonal structures. The requirement of structural stability criteria [34, 35] in all structures leads to the following limitations in elastic constants: For cubic structure: $C_{11}–C_{12} > 0$, $C_{44} > 0$, $C_{11} + 2C_{12} > 0$ and $C_{12} < B < C_{11}$, for tetragonal: $C_{11} > 0$, $C_{33} > 0$, $C_{44} > 0$, $C_{66} > 0$, $(C_{11}–C_{12}) > 0$, $(C_{11} + C_{33}–2C_{13}) > 0$.

The elastic calculations of $Mn_2Cr_{1-x}V_xSi$ ($x = 0, 0.25, 0.5, 0.75, 1$) alloys are calculated by applying stress to the optimized crystal structure. The elastic constant values calculated for cubic and tetragonal alloys are presented in Table 2. It can be clearly seen in Table 2 that the studied alloys in all structures have mechanical stability because of the satisfaction of Born stability criteria. When the C_{11} value of the elastic constants of these alloys is considered, it is understood that as the contribution of the V atom increases, the C_{11} value increases, but in the absence of the Cr atom, it decreases as in the Mn_2VSi alloy. In the C_{12} value, it is seen that the cubic alloys are similar to the result in C_{11} with the V contribution among themselves. The C_{44} values of these alloys vary slightly with the contribution of the V atom for all alloys.

The important mechanical properties of materials such as bulk modulus, shear modulus, Young modulus, Poisson's ratio, anisotropic factor, brittle/ductile behavior or hardness and Debye or melting temperature are also calculated from elastic constants using the Voigt–Reuss–Hill approach [36–40] and presented in Table 3.

Bulk modulus values of these alloys have been obtained at a value between C_{11} and C_{12} elastic constant values, as expected. In the Shear modulus, which is another expression of compressibility, it was understood that these alloys are less compressible since they have a value above 100 GPa. It was also observed that the shear modulus value increased as the contribution of the V atom increased. Pugh's criterion, which is used to obtain information about the brittle or ductile nature of materials, is one of the most widely used criteria [41]. According to this criterion, the material has a brittle nature if the B/G ratio is less than 1.75, and ductile if it is higher than 1.75. Accordingly, Mn_2VSi alloy with a B/G ratio less than 1.75 value has a brittle nature, while other alloys have a ductile nature because it is greater than 1.75 value. When the Young modulus, which is another expression of hardness, is investigated, it is seen in Table 3 that the Young modulus increases with the increase in V contribution in alloys found in ductile nature. This result is consistent with the result of Vickers hardness values, but considering the additive ratio $x = 1$, the Mn_2VSi alloy is the hardest among these alloys. In other words, if one thinks that hard materials have a more brittle structure, it can be said that the materials become harder with the addition of V atoms. For these anisotropic alloys, the Young modulus, compressibility and shear modulus minimum and maximum values were calculated using ELATE codes [42] and given in Table 4.

The calculated Poisson's ratio generally contains information about atomic bonding. The value of Poisson's ratio

Table 1 Atomic Wyckoff positions of the studied alloys

Materials	Mn	Cr	V	Si
Mn_2CrSi	0.25 0.25 0.25	0.50 0.50 0.50	–	0 0 0
$Mn_2Cr_{0.75}V_{0.25}Si$	0.25 0.25 0.25	0.50 0 0	0.50 0.50 0.50	0 0 0
	0.25 0.25 0.75			0 0.50 0.50
	0.75 0.75 0.25			
$Mn_2Cr_{0.5}V_{0.5}Si$	0 0.50 0.25	0.50 0.50 0	0 0 0.50	0 0 0
				0.50 0.50 0.50
$Mn_2Cr_{0.25}V_{0.75}Si$	0.25 0.25 0.25	0.50 0.50 0.50	0.50 0 0	0 0 0
	0.25 0.25 0.75			0 0.50 0.50
	0.75 0.75 0.25			
Mn_2VSi	0.25 0.25 0.25	–	0.50 0.50 0.50	0 0 0

Table 2 Lattice constants a_0, c (Å), bulk modulus B (GPa) and elastic constants C_{ij} (GPa) of $Mn_2Cr_{1-x}V_xSi$ (x = 0; 0.25; 0.5; 0.75; 1) alloys

Materials	*Ref.*	a_0	c	B	C_{11}	C_{12}	C_{44}	C_{13}	C_{33}	C_{66}
Mn_2CrSi	This work	5.593	–	242.63	385.10	171.40	132.09	–	–	–
	FLAPW [15]	5.590								
	FLAPW [16]	5.623								
$Mn_2Cr_{0.75}$ $V_{0.25}Si$	This work	5.606	–	262.01	414.55	185.74	137.66	–	–	–
$Mn_2Cr_{0.5}$ $V_{0.5}Si$	This work	3.973	5.615	261.31	441.00	154.67	145.03	183.13	428.34	117.33
$Mn_2Cr_{0.25}$ $V_{0.75}Si$	This work	5.636	–	261.74	416.58	184.32	147.27	–	–	–
Mn_2VSi	This work	5.652	–	220.96	373.49	144.69	150.69	–	–	–
	FPLO [18]	5.560								

Table 3 Calculated bulk modulus B (GPa), shear modulus G (GPa), young modulus E (GPa), Vickers hardness H_v, B/G ratio, Poisson's ratio σ, anisotropy factor A, Debye temperature θ_D (K) and melting temperature T_{melt} (K) of $Mn_2Cr_{1-x}V_xSi$ (x = 0; 0.25; 0.5; 0.75; 1) alloys

Materials	*Ref.*	B	G	B/G	E	H_v	σ	A	θ_D	T_{melt}
Mn_2CrSi	This work	242.63	121.34	2.00	312.01	14.73	0.286	1.236	612.95	2829 ± 300
	CASTEP [20]	–	–	5.78	–		0.30	–		
$Mn_2Cr_{0.75}$ $V_{0.25}Si$	This work	262.01	127.83	2.05	329.86	14.75	0.290	1.203	630.79	3003 ± 300
$Mn_2Cr_{0.5}$ $V_{0.5}Si$	This work	261.31	133.48	1.96	342.17	15.96	0.282	1.236	644.92	3159 ± 300
$Mn_2Cr_{0.25}$ $V_{0.75}Si$	This work	261.74	133.91	1.95	343.20	16.02	0.281	1.268	647.26	3012 ± 300
Mn_2VSi	This work	220.96	134.95	1.64	336.37	19.80	0.246	1.317	648.08	2760 ± 300
	CASTEP [20]	–	–	1.69	–		0.25	–		

is close to 0.1 in covalent materials and close to 0.25 in ionic materials [32, 43]. Since the calculated Poisson's ratios of these alloys are in the range of 0.24–0.29, it can be said that they have an ionic character. Another parameter obtained within the scope of mechanical properties of materials is the anisotropy factor. The anisotropy factor is equal to 1 for isotropic materials, and it is different from 1 for anisotropic materials. Accordingly, the anisotropy factors of the studied alloys here have greater than 1. Therefore, it can be said that alloys are anisotropic. In addition, to define the anisotropy of these alloys more clearly, we have investigated the dependence of Young modulus in the three-dimensional (3D) direction and the two-dimensional (2D) direction of the alloys. The 3D and 2D surface

Table 4 Maximum and minimum values of young modulus, compressibility and shear modulus of $Mn_2Cr_{1-x}V_xSi$ (x = 0; 0.25; 0.5; 0.75; 1) alloys

Malzemeler	E_{min}	E_{max}	β_{min}	β_{max}	G_{min}	G_{max}
Mn_2CrSi	279.52	335.40	1.373	1.373	106.85	132.09
$Mn_2Cr_{0.75}$ $V_{0.25}Si$	299.61	351.44	1.272	1.272	114.41	137.66
$Mn_2Cr_{0.5}$ $V_{0.5}Si$	305.85	366.04	1.219	1.303	117.33	145.03
$Mn_2Cr_{0.25}$ $V_{0.75}Si$	303.50	372.04	1273	1.273	116.13	147.27
Mn_2VSi	292.69	368.34	1.508	1.508	114.40	150.69

structures of the Young modulus of the considered alloys are shown in Fig. 2. A spherical shape for 3D and a circular shape for 2D indicate an isotropic system, while possible deviations from sphericity describe the degree of anisotropy. It is clearly seen in Fig. 2 that the surface shapes are far from spherical from 2 and 3D graphs of the Young modulus. Thus, all alloys indicate an anisotropic character.

The equilibrium lattice constants of these alloys obtained within the structural properties have been used to calculate the magnetic and electronic properties. Considering the spin contribution, the calculations have been made according to spin polarizations to form ferrimagnetic material for $Mn_2Cr_{1-x}V_xSi$ (x = 0, 0.25, 0.5, 0.75, 1) alloys. While the total magnetic moments for $Mn_2Cr_{1-x}V_xSi$ (x = 0.25, 0.50 and 0.75) were zero, they were obtained as 0.23 and 0.41 μB for $Mn_2Cr_{1-x}V_xSi$ (x = 0 and 1), respectively. From the magnetic calculations, it was concluded that $Mn_2Cr_{1-x}V_xSi$ (x = 0.25, 0.50 and 0.75) alloys are non-magnetic and have a very small magnetization for $Mn_2Cr_{1-x}V_xSi$ (x = 0 and 1) alloys.

The spin polarization electronic band energy curves and their partial and total state densities have been plotted and presented in Figs. 3 and 4. When the electronic band curves in Fig. 3 are analyzed in terms of the electronic properties, there is no band gap between the valence and conduction bands in the Fermi level in the spin-up and spin-down orientation of all alloys. Thus, both spin-up and spin-down states of all alloys exhibit metallic character.

To investigate the total and partial state densities and to better determine the contribution to the conductivity from each element of these alloys, in the spin-up and spin-down directions, it is seen that the main contribution in the Fermi level of the electrons belonging to the atoms forming the alloys is from the Mn-3d and Cr-3d (V-3d) orbitals. However, in $Mn_2Cr_{1-x}V_xSi$ (x = 0, 0.25, 0.5, 0.75 and 1) alloys, the electrons of the Mn-3d orbital are most dominant. At the same time, it can be seen from the figures that as the doping ratio of the V atom in the alloy increases, the contribution from the electrons of the Cr-3d orbital decreases. In addition, when the electronic properties of these alloys were compared with the studies in the literature, they were found to be compatible.

Thermodynamic calculations have been done for $Mn_2Cr_{1-x}V_xSi$ (x = 0, 0.25, 0.5, 0.75 and 1) alloys using the Debye model by applying stress to the optimized crystal structure. Various thermodynamic properties such as internal energy, vibrational energy, entropy and specific heat capacity for $Mn_2Cr_{1-x}V_xSi$ (x = 0, 0.25, 0.5, 0.75 and 1) alloys have been investigated and evaluated depending on temperature in the range of 0–800 K and presented in Fig. 5. When the change of entropy depending on temperature is examined, it is seen that the entropy increases with the increase in temperature, as expected. It is also seen that the temperature-related entropy increase is the highest in the x = 0.25 and 0.75 V atom doped states in the Pm-3m space group, and the least in the x = 0 and 1 V states in the Fm-3m space group. Examining the variation of the heat capacity with temperature, It is noticed that the heat capacity increases as the temperature increases and approaches the value of $3NR$ (number of atoms in N unit cell, R gas constant) known as the Dulong–Petit limit [44] when going toward high temperatures. It is found that the heat capacity of the alloys at x = 0.25 and 0.75 in the Pm-3m space group with 16 atoms in the unit cell is high. The Debye temperature, which is also known as the place where the heat capacity starts to flatten and the temperature value at which the materials reach the highest vibration frequency, is 612.94, 630.79, 644.92, 647.26 and 648.07 K that were calculated for $Mn_2Cr_{1-x}V_xSi$ (x = 0, 0.25, 0.5, 0.75 and 1) alloys, respectively. In addition, considering the calculated melting temperatures of these alloys, it is seen that they have the highest melting temperature at the x = 0.50 additive ratio and the lowest melting temperature at the x = 1 additive ratio. It can be said that these alloys are suitable for use as high-temperature materials at melting temperatures. When examining the variation of vibration energy, which is another thermodynamic property, depending on temperature, it is clearly seen that the vibration energy in alloys increases with the increase in temperature. However, in the case of examining the

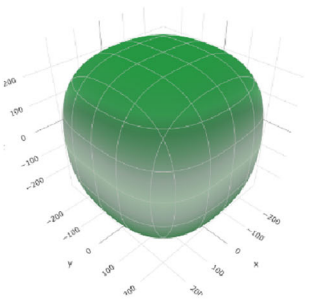

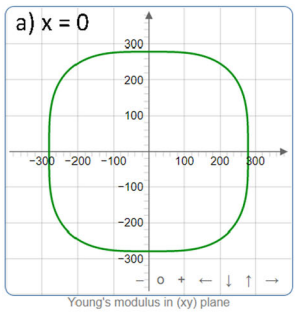
a) x = 0
Young's modulus in (xy) plane

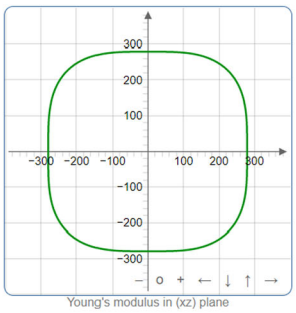
Young's modulus in (xz) plane

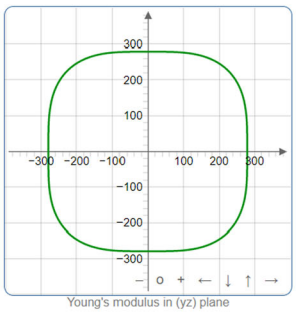
Young's modulus in (yz) plane

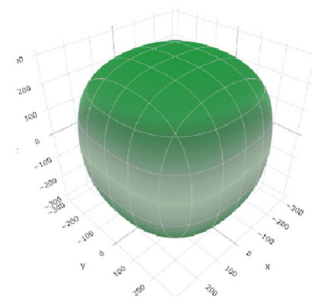

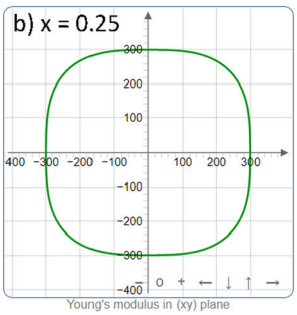
b) x = 0.25
Young's modulus in (xy) plane

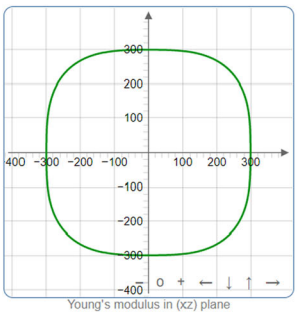
Young's modulus in (xz) plane

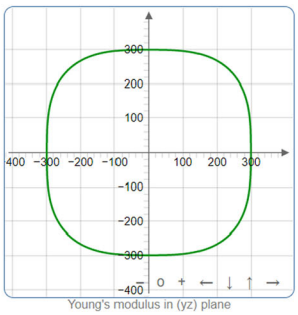
Young's modulus in (yz) plane

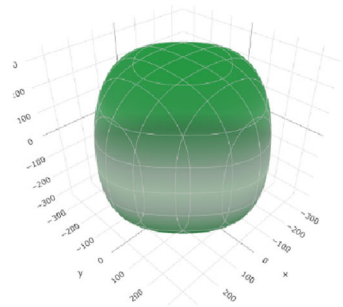

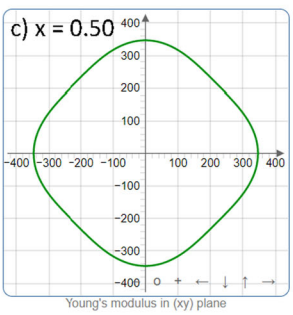
c) x = 0.50
Young's modulus in (xy) plane

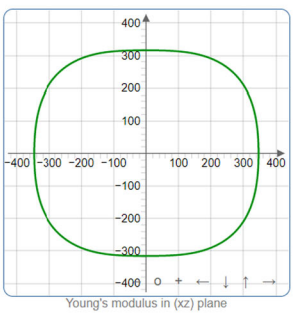
Young's modulus in (xz) plane

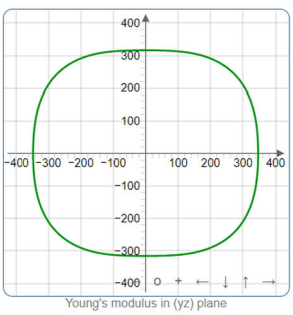
Young's modulus in (yz) plane

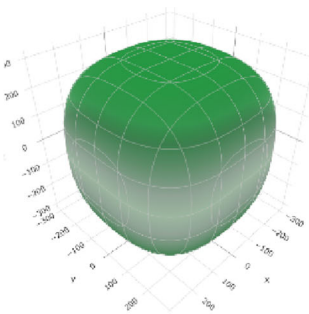

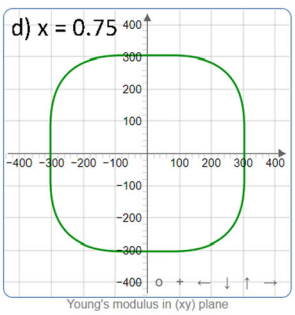
d) x = 0.75
Young's modulus in (xy) plane

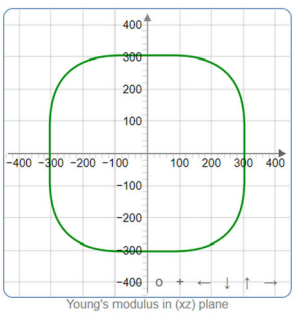
Young's modulus in (xz) plane

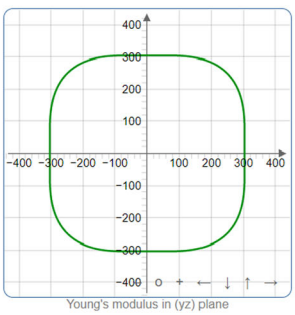
Young's modulus in (yz) plane

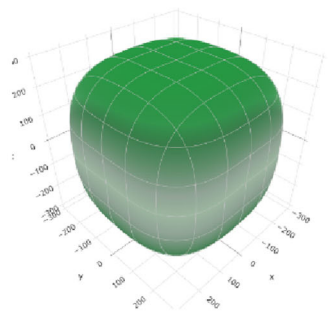

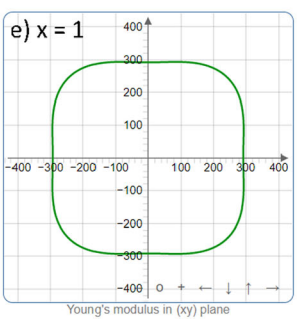
e) x = 1
Young's modulus in (xy) plane

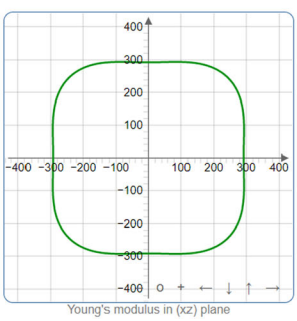
Young's modulus in (xz) plane

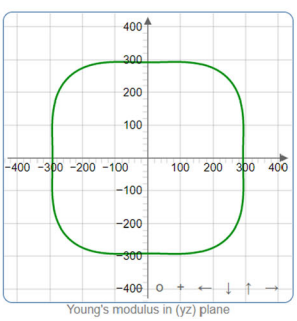
Young's modulus in (yz) plane

◀**Fig. 2** 3D and 2D directional change of Young Modulus of $Mn_2Cr_{1-x}V_xSi$ (x = 0; 0.25; 0.5; 0.75; 1) alloys

variation of vibration free energy with temperature, it is noticed that there is a decrease inversely proportional to the temperature increase. The increase in vibration energy in the materials with the increase in temperature causes a decrease in the vibration free energy as expected. Therefore, at x = 0.25, 0.75 V cases, it is observed that the vibration energy increases the most depending on the temperature, and the vibration free energy decreases the most with the temperature increase.

One of the powerful ways to reveal the structural stability of materials is through the calculation of phonon dispersion curves. First, we check the dynamic stability of

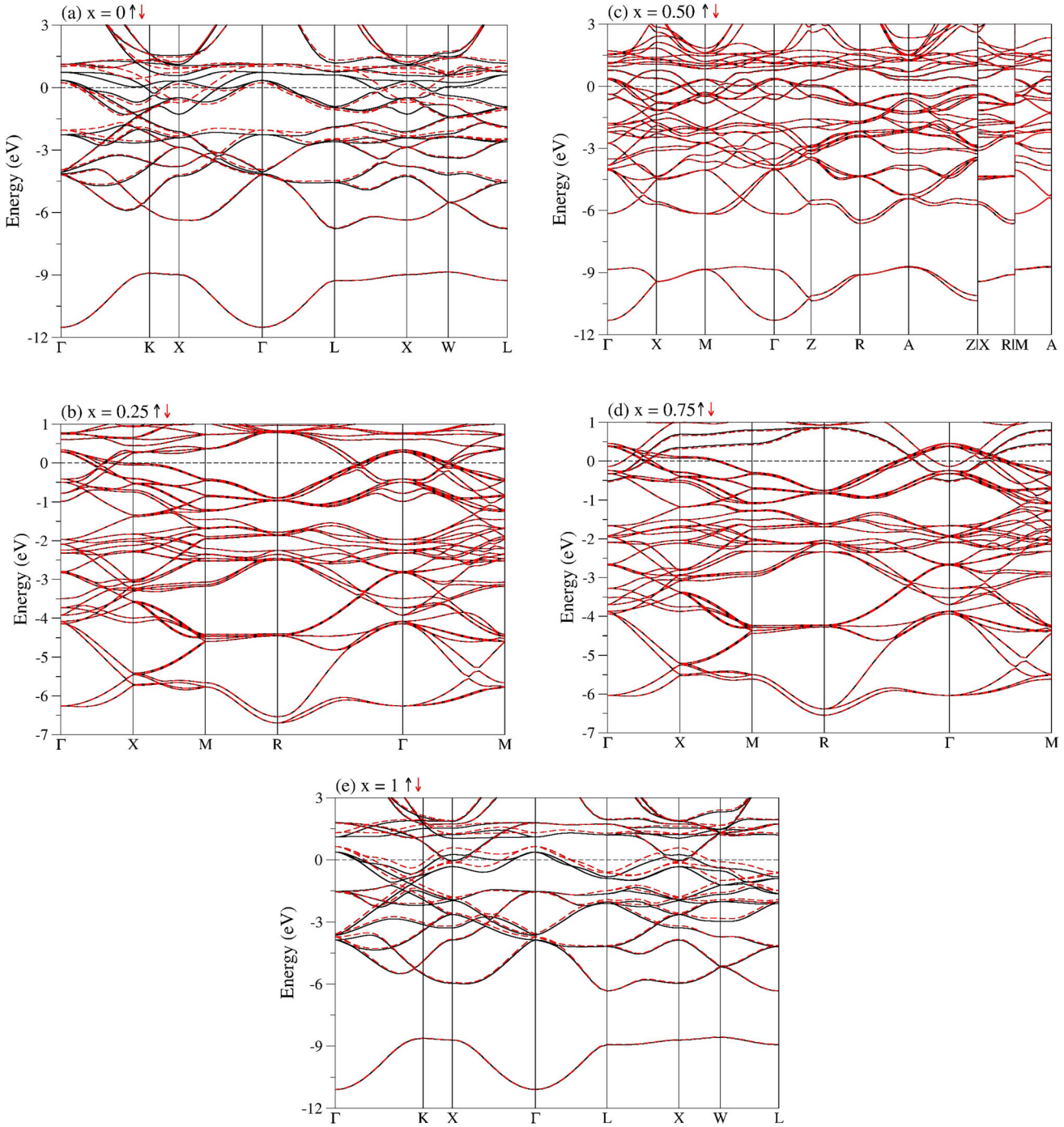

Fig. 3 Spin-polarized band structures of $Mn_2Cr_{1-x}V_xSi$ (x = 0; 0.25; 0.5; 0.75; 1) alloys

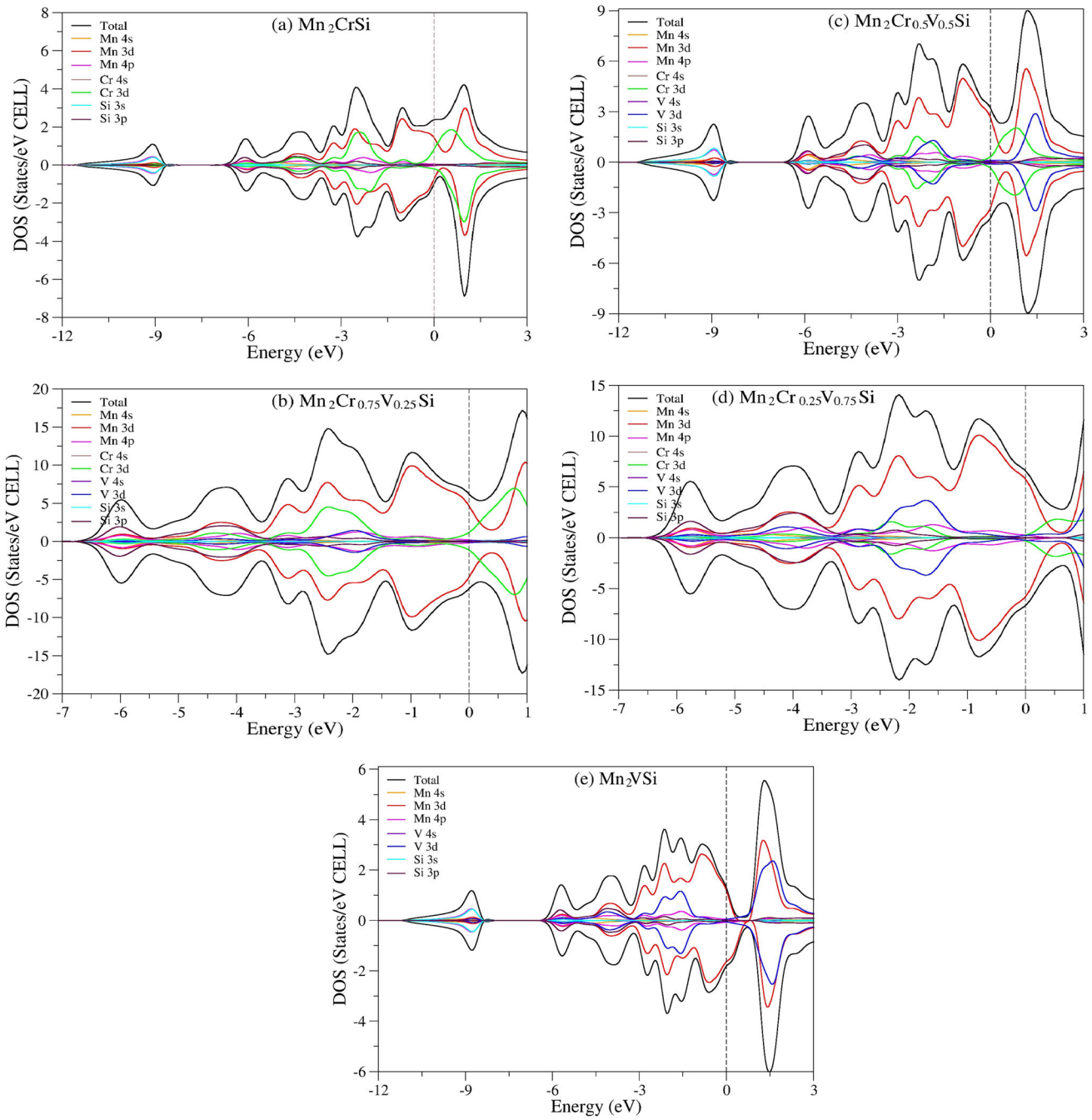

Fig. 4 Spin-polarized total and partial density of states (DOS) of $Mn_2Cr_{1-x}V_xSi$ (x = 0; 0.25; 0.5; 0.75; 1) alloys

full-Heusler $Mn_2Cr_{1-x}V_xSi$ (x = 0 and 1) alloys using the vibrational phonon spectrum. The calculated phonon dispersion curves and projected density of states of $Mn_2Cr_{1-x}V_xSi$ (x = 0 and 1) alloys have been shown in Fig. 6. $Mn_2Cr_{1-x}V_xSi$ (x = 0 and 1) alloys contain four atoms in their primitive unit cell. Thus, there are twelve phonon branches available, three of which are acoustic and the remaining nine are optical modes. Figure 6(a and b) shows typical phonon spectra with two transverse acoustic branches and one longitudinal acoustic branch clearly presented. All phonon modes are positive along the Brillouin zone, indicating that $Mn_2Cr_{1-x}V_xSi$ (x = 0 and 1) is dynamically stable. Also, a band gap separating the top optical phonon modes from other optical modes is quite remarkable. Band gaps in the phonon spectrum can often be associated with thermal conductivity [45–50]. The larger the gap between acoustic and optical phonons, the higher the thermal conductivity. Unfortunately, there are

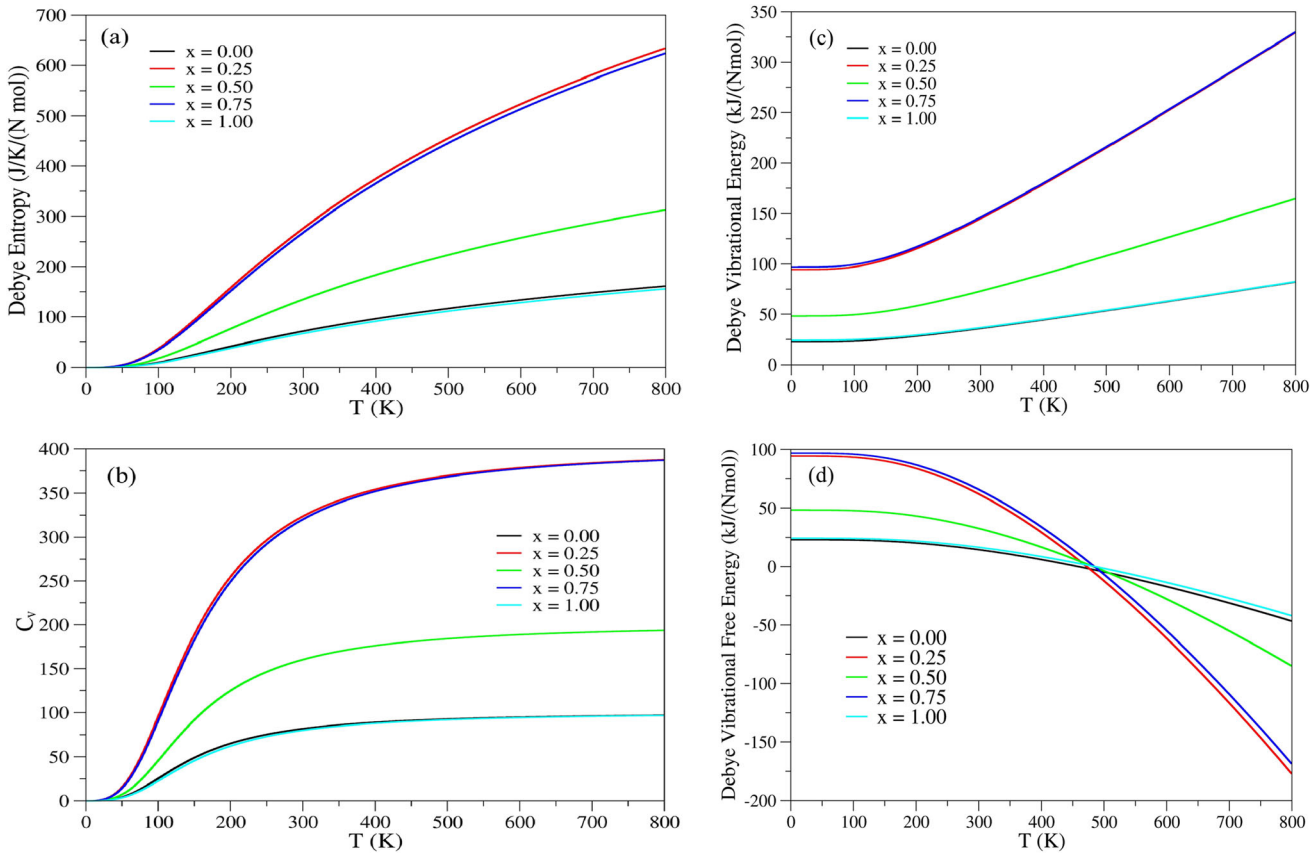

Fig. 5 (a) Entropy change, (b) Specific heat capacity at constant volume, (c) Debye vibrational energy and (d) Debye vibrational free energy with temperature for $Mn_2Cr_{1-x}V_xSi$ (x = 0; 0.25; 0.5; 0.75; 1) alloys

no experimental or theoretical results with which the calculated phonon spectra can be compared in the literature.

4. Conclusions

In this study, structural, electronic, magnetic and mechanical properties of alloys in the form of $Mn_2Cr_{1-x}V_xSi$ (x = 0, 0.25, 0.5, 0.75 and 1) by doping V atom to Mn_2CrSi full-Heusler alloy have been calculated using the density functional theory scheme within a generalized gradient approximation. In all calculations for these alloys, x = 0; In the full-Heusler structure in the Fm-3m space group in the case of 1 doping, x = 0.25; It was done by keeping the positions of the atom's constant in the simple cubic structure in the Pm-3m space group in the 0.75 doping state and the tetragonal structure in the P/4mmm space group in the x = 0.50 doping state.

The results of the calculations are as follows:

Within the scope of structural features:

- The lattice constants of Mn_2CrSi and Mn_2VSi complete Heusler alloys in the Fm-3m space group were calculated as 5.593 and 5.652 Å, respectively.
- In the cubic structure of $Mn_2Cr_{0.25}V_{0.75}Si$ and $Mn_2Cr_{0.25}V_{0.75}Si$ alloys in the Pm-3m space group, the lattice constants were calculated as 5.606 and 5.636 Å, respectively.
- The lattice constants of the $Mn_2Cr_{0.5}V_{0.5}Si$ tetragonal alloy in the P4/mmm space group were calculated as a = 3.974 Å and c = 5.615 Å.
- The lattice constant values of Mn_2CrSi and Mn_2VSi full-Heusler alloys were compared with the studies in the literature, and it was seen that they were quite compatible. For other alloys, a comparison could not be made since no study was found in the literature.

Within the scope of magnetic properties:

- In this study, the spin orientations of these alloys were preferred according to the ferrimagnetic structure, and calculations were done according to the spin-down and spin-up states. Total magnetic moments were obtained as zero at x = 0.25, 0.50 and 0.75 doping cases, 0.23 μ_B at x = 0, and 0.41 μ_B at x = 1. From the magnetic property calculations, it was concluded that these alloys were not magnetic at x = 0.25, 0.50 and 0.75 doping

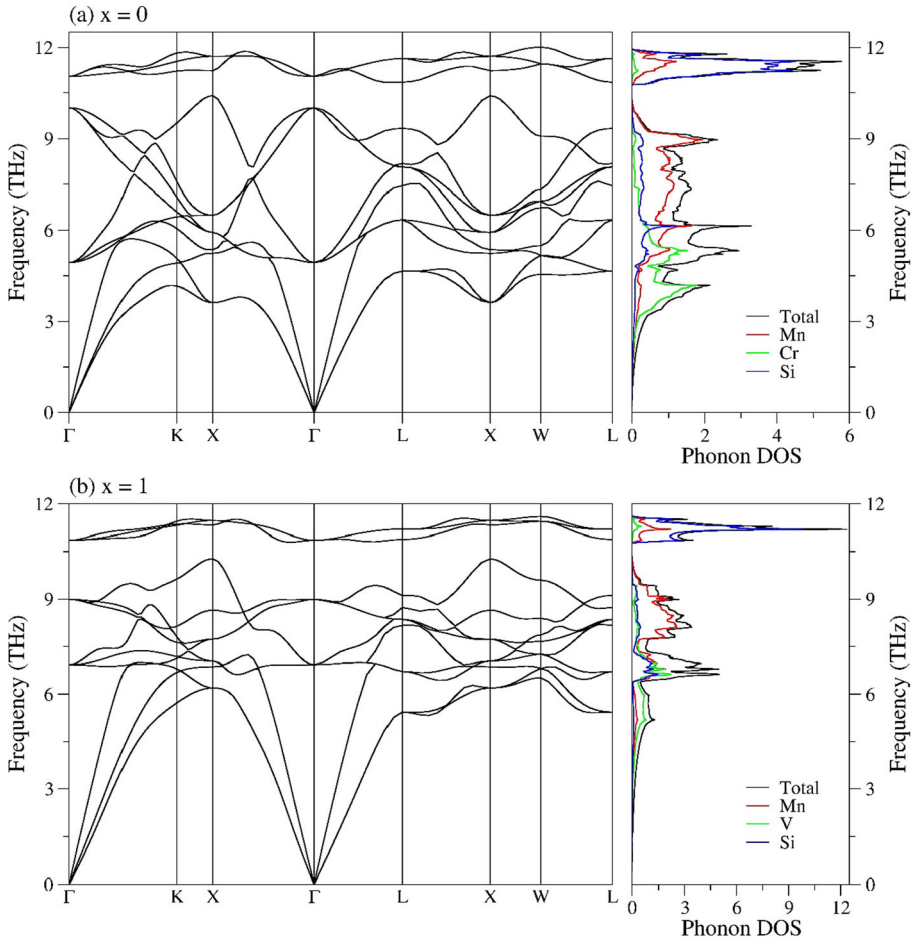

Fig. 6 Phonon dispersion curves and state densities for $Mn_2Cr_{1-x}V_xSi$ (x = 0 and 1) alloys

states and had a very small magnetization for x = 0 and 1 doping states.

Within the scope of electronic features:

- It was understood that each of these alloys, whose electronic band curves and state densities were calculated according to spin polarization, had a metallic character.
- It was seen that the highest contribution to the conductivity of these alloys, whose total and partial state densities were calculated, came from Mn-3d. In addition, it was understood that the contribution of Cr-3d to the conductivity decreased as the doping ratio of the V atom increased.

Within the scope of mechanical properties:

- Second order elastic constants and polycrystalline properties of $Mn_2Cr_{1-x}V_xSi$ (x = 0, 0.25, 0.5, 0.75, 1) alloys were obtained.
- From the obtained elastic constants, these alloys were found to be mechanically stable.
- It was understood from the calculated Bulk, Shear and Young modulus that their compressibility was low.
- From the *B/G* ratios, it was seen that the Mn_2VSi full-Heusler alloy has a brittle nature, while the other alloys have a ductile nature.
- Considering the boundary conditions of these alloys with Poisson's ratio, it was concluded that they have an ionic-metallic characterization.
- It was found that the hardness of these alloys increased as the V contribution of the Vickers hardness values increased. In addition, these alloys are hard materials.

Within the scope of thermodynamic properties:

- Using the semi-harmonic Debye model, temperature-dependent changes of entropy, heat capacity, vibrational energy and vibrational free energy were calculated for $Mn_2Cr_{1-x}V_xSi$ (x = 0, 0.25, 0.5, 0.75, 1) alloys.
- Debye temperatures for $Mn_2Cr_{1-x}V_xSi$ (x = 0, 0.25, 0.5, 0.75, 1) alloys were obtained as 612,949, 630,792, 644.921, 647.263 and 648.076 K, respectively.
- It was determined that $Mn_2Cr_{0.5}V_{0.5}Si$ alloy had the highest melting temperature from the calculated melting temperatures of these alloys, and Mn_2VSi alloy had the lowest melting temperature.

There is no study in the literature about $Mn_2Cr_{1-x}V_xSi$ (x = 0, 0.25, 0.5, 0.75, 1) alloys calculated in this study, except for Mn_2CrSi and Mn_2VSi alloys, and this study shows that these alloys are structural, electronic, magnetic, mechanical and thermodynamic properties that have been brought to the literature. However, there is a need for many more experimental and theoretical studies on all of these alloys.

References

[1] F Heusler *Verhandlungen der Deutschen Physikalischen Gesellschaft* **5** 219 (1903)
[2] J Vondrášek, L Bendová, V Klusák and P Hobza *Journal of the American Chemical Society* **127** 2615 (2005)
[3] S Grimme *Journal of Computational Chemistry* **25** 1463 (2004)
[4] U Zimmerli, M Parrinello and P Koumoutsakos *Journal of Chemical Physics* **120** 2693 (2004)
[5] M G Medvedev, I S Bushmarinov, J Sun, J P Perdew and K A Lyssenko *Science* **355** 49 (2017)
[6] H Jiang *The Journal of Chemical Physics* **138** 134115 (2013)
[7] D Bagayoko *AIP Advances* **4** 127104 (2014)
[8] M Brack *Physical Review D* **27** 1950 (1983)
[9] K Koshelev *arXiv preprint* arXiv:0812.2919 (2008)
[10] W Kohn and L J Sham *Physical Review* **140** A1133 (1965)
[11] R G Parr and W Yang *Density-Functional Theory of Atoms and Molecules* (Oxford University Press) (1994)
[12] W C Topp and J J Hopfield *Physical Review B* **7** 1295 (1973)
[13] C F Fischer *Computer Physics* Communications **43** 355 (1987)
[14] I N Levine *Quantum Chemistry* (eds) E. Cliffs (New Jersey: Prentice Hall) p 403 (1991)
[15] H Luo, Z Zhu, G Liu, S Xu, G Wu, H Liu, J Qu and Y Li *Journal of Magnetism and Magnetic Materials* **320** 421 (2008)
[16] S Fujii, M Okada, S Ishida and S Asano *Journal of the Physical Society of Japan* **77** 074702 (2008)
[17] H Wu, G Vallejo-Fernandez and A Hirohata *Journal of Physics D: Applied Physics* **50** 375001 (2017)
[18] K Özdoğan, I Galanakis, E Şaşıoğlu and B Aktaş *Journal of Physics: Condensed Matter* **18** 2905 (2006)
[19] I Galanakis, K Özdoğan, E Şaşıoğlu and B Aktaş *Physical Review B* **75** 092407 (2007)
[20] Y Li, J Zhu, R Paudel, J Huang and F Zhou *Computational Materials Science* **193** 110391 (2021)
[21] S Kirklin, J E Saal, V I Hegde and C Wolverton *Acta Materialia* **102** 125 (2016)
[22] I Asfour, H Rached, S Benalia and D Rached *Journal of Alloys and Compounds* **676** 440 (2016)
[23] I Asfour, H Rached, D Rached, M Caid and M Labair *Journal of Alloys and Compounds* **742** 736 (2018)
[24] O Cheref et al. *Computational Condensed Matter* **19** e00369 (2019)
[25] Y Rached, M Caid, M Merabet, S Benalia, H Rached, L Djoudi, M Mokhtari and D Rached *International Journal of Quantum Chemistry* **122** e26875 (2022)
[26] A A Mousa et al. *Materials Chemistry and Physics* **249** 123104 (2020)
[27] M Çanlı, E Ilhan and N Arıkan *Materials Today Communications* **26** 101855 (2021)
[28] W Kohn *Physical Review Letters* **76** 3168 (1996)
[29] P Giannozzi, S Baroni, N Bonini, et al *Journal of Physics: Condensed Matter* **21** 395502 (2009)
[30] P Perdew, K Burke and M Ernzerhof *Physical Review Letters* **77** 3865 (1996)
[31] M Methfessel and A T Paxton *Physical Review B* **40** 3616 (1989)
[32] O H Nielsen and R M Martin *Physical Review Letters* **50** 697 (1983)
[33] P Giannozzi et al *Journal of Physics: Condensed Matter* **29** 465901 (2017)
[34] M Born and K Huang *Dynamical Theory of Crystal Lattices* (Oxford: Clarendon) (1954)
[35] A. Bouhemadou and R Khenata *Physics Letters A* **362** 476 (2007)
[36] A Maachou, H Aboura, B Amrani, R Khenata, S B Omran and D Varshney *Computational Materials Science* **50** 3123 (2011)
[37] M Moakafi, R Khenata, A Bouhemadou, F Semari, A H Reshak and M Rabah *Computational Materials Science*, **46** 1051 (2009)
[38] W Voigt *Lehrburch der Kristallphysik* (Teubner, Leipzig) (1928)
[39] A Reuss *Journal of Applied Mathematics and Mechanics/ Zeitschrift für Angewandte Mathematik und Mechanik* **9** 49 (1929)
[40] R Hill *Proceedings of the Physical Society. Section A* **65** 349 (1952)
[41] S F Pugh *Dublin Philosophical Magazine and Journal of Science* **45** 823 (1954)
[42] R Gaillac, P Pullumbi and F X Coudert *Journal of Physics: Condensed Matter* **28** 275201 (2016)
[43] F. Mouhat and F.X. Coudert *Physical Review B* **90** 224104 (2014)
[44] A T Petit and P L Dulong *Annales de Chimie et de Physique* **10** 395 (1819)
[45] S Al *International Journal of Hydrogen Energy* **44** 1727 (2019)
[46] S Al, N Arıkan and A İyigör *Zeitschrift für Naturforschung A* **73** 859 (2018)
[47] S Al and A İyigör *Chemical Physics Letters* **743** 137184 (2020)
[48] L Lindsay and D A Broido *Journal of Physics: Condensed Matter.* **20** 165209 (2008)
[49] A İyigör, S Al and N Arıkan *Chemical Physics Letters* **806** 140052 (2022)
[50] N Arıkan, H Y Ocak, G Dikici Yıldız, Y G Yıldız and R Ünal *Journal of the Korean Physical Society* **76** 916 (2020)

Publisher's Note Springer Nature remains neutral with regard to jurisdictional claims in published maps and institutional affiliations.

Springer Nature or its licensor (e.g. a society or other partner) holds exclusive rights to this article under a publishing agreement with the author(s) or other rightsholder(s); author self-archiving of the accepted manuscript version of this article is solely governed by the terms of such publishing agreement and applicable law.